HHS Public Access

Author manuscript

Oncogene. Author manuscript; available in PMC 2017 July 25.

Published in final edited form as:

Oncogene. 2017 July 06; 36(27): 3878–3889. doi:10.1038/onc.2017.14.

LncRNA *MEG3* Downregulation Mediated by DNMT3b Contributes to Nickel Malignant Transformation of Human Bronchial Epithelial Cells *via* Modulating PHLPP1 Transcription and HIF-1α Translation

Chengfan Zhou[1,2,3,¶], **Chao Huang**[3,¶], **Jingjing Wang**[3], **Haishan Huang**[2], **Jingxia Li**[3], **Qipeng Xie**[2], **Yu Liu**[4], **Junlan Zhu**[3], **Yang Li**[3], **Dongyun Zhang**[3], **Qixing Zhu**[1,*], and **Chuanshu Huang**[2,3,*]

[1]Department of Occupational and Environmental Health, School of Public Health, Anhui Medical University, Hefei, Anhui 230032, China

[2]Zhejiang Provincial Key Laboratory for Technology & Application of Model Organisms, School of Life Sciences, Wenzhou Medical University, Wenzhou, Zhejiang 325035, China

[3]Nelson Institute of Environmental Medicine, New York University School of Medicine, Tuxedo, NY 10987, USA

[4]Department of Cardiothoracic Surgery, The First Affiliated Hospital, Wenzhou Medical University, Wenzhou, Zhejiang 325035, China

Abstract

Long noncoding RNAs (lncRNAs) are emerging as key players in various fundamental cellular biological processes, and many of them are likely to have functional roles in tumorigenesis. Maternally expressed gene 3 (*MEG3*) is an imprinted gene located at 14q32 that encodes an lncRNA, and the decreased *MEG3* expression has been reported in multiple cancer tissues. However, nothing is known about the alteration and role of *MEG3* in environmental carcinogen-induced lung tumorigenesis. Our present study, for the first time to the best of our knowledge, discovered that environmental carcinogen nickel exposure led to *MEG3* downregulation, consequently initiating c-Jun-mediated PHLPP1 transcriptional inhibition and hypoxia-inducible

[*]**Corresponding author**: Dr. Chuanshu Huang, Nelson Institute of Environmental Medicine, New York University School of Medicine, 57 Old Forge Road, Tuxedo, NY 10987, USA, Tel: 845-731-3519, Fax: 845-351-2320, chuanshu.huang@nyumc.org, Dr. Qixing Zhu, zqxing@yeah.net.

[¶]These authors contributed equally to this work.

Conflicts of interest: The authors declare no conflict of interest.

Authors' Contributions

Conception and design: C. Zhou, Q. Zhu, C. Huang

Acquisition of data (acquired and managed patients, provided facilities, etc.): C. Zhou, H. Huang, J. Li, Q. Xie, J. Zhu, Y. Li, D. Zhang, Y. Liu, and J. Wang

Analysis and interpretation of data (e.g., statistical analysis, biostatistics, computational analysis): C. Zhou, H. Huang, and C. Huang

Writing, review, and revision of the manuscript: C. Zhou and C. Huang

Administrative, technical, or material support (i.e., reporting or organizing data, constructing databases): C. Zhou, J. Li, Q. Zhu, and C. Huang

Study supervision: C. Huang

Supplemental Information

Supplemental Material is available online

factor-1α (HIF-1α) protein translation upregulation, in turn resulting in malignant transformation of human bronchial epithelial cells. Mechanistically, *MEG3* downregulation was attributed to nickel-induced promoter hypermethylation *via* elevating DNMT3b expression, while PHLPP1 transcriptional inhibition was due to the decreasing interaction of *MEG3* with its inhibitory transcription factor c-Jun. Moreover, HIF-1α protein translation was upregulated *via* activating the Akt/p70S6K/S6 axis resultant from PHLPP1 inhibition in nickel responses. Collectively, we uncover that nickel exposure results in DNMT3b induction and *MEG3* promoter hypermethylation and expression inhibition, further reduces its binding to c-Jun and in turn increasing c-Jun inhibition of PHLPP1 transcription, leading to the Akt/p70S6K/S6 axis activation, and HIF-1α protein translation as well as malignant transformation of human bronchial epithelial cells. Our studies provide a significant insight into understanding the alteration and role of *MEG3* in nickel-induced lung tumorigenesis.

Keywords

LncRNA *MEG3*; DNMT3b; PHLPP1; HIF-1α translation; Nickel

Introduction

Lung cancer is the leading cause of cancer mortality around the world with an estimated 89,320 and 73,190 deaths predicted to occur in men and women, respectively, in 2016 in the United States[1]. Although, lung cancer cases are attributable in part to smoking tobacco, environmental pollution is more likely cause nonsmoking-related lung cancer[2]. Therefore, understanding the environmental factors that predispose an individual to nonsmoking-related lung cancer is of prime importance. Nickel is one of the most common environmental factors and is considered to be a group 1 human carcinogen by the International Agency Research on Cancer (IARC) in 1990[3]. The carcinogenic action of nickel compounds is thought to involve oxidative stress, epigenetic effects, and the regulation of gene expression by activation of certain transcription factors related to corresponding signal transduction pathways[4]. Hypoxia-inducible factor-1 (HIF-1) is a heterodimeric transcription factor that plays a key role in cellular adaptations to hypoxia by controlling the expression of a series of genes involved in angiogenesis, oxygen transport, and glucose metabolism[5]. HIF-1 consists of HIF-1α and HIF-1β (also known as aryl hydrocarbon nuclear receptor translocator, ARNT). Both HIF-1α and HIF-1β are required for formation of the HIF-1 heterodimer, whereas HIF-1α is a key regulatory subunit and is responsible for HIF-1 transcriptional function[6]. Our previous studies indicate that nickel exposure results in HIF-1α protein accumulation[7–10], consequently contributing to cell transformation[9]. However, the molecular mechanisms underlying the HIF-1α protein accumulation upon nickel exposure are far from fully understood although it is well-known that the inhibition of HIF-1α protein degradation is involved.

Long noncoding RNAs (lncRNAs) are a heterogeneous group of non-coding transcripts longer than 200 nucleotides. Abnormal expression of many lncRNAs has been reported to be involved in cancer predisposition, development, and progression[11]. Maternally expressed gene 3 (*MEG3*) is an lncRNA with a length of ~1.6 kb nucleotides and is reciprocally

imprinted with the paternally expressed gene DLK1 constituting an imprinting domain on human chromosome 14q32 [12]. In humans, *MEG3* is expressed in many normal tissues[13], while the loss of *MEG3* expression has been found in various types of tumor tissues and cell lines, which are associated with tumor development and progression[14]. However, the role of *MEG3* in environmental carcinogen-induced lung cancer remains largely unknown.

Epigenetic mechanisms have been well known for their contribution to the carcinogenic characteristics of nickel [15], and multiple epigenetic mechanisms have been identified that mediate gene silencing following nickel exposure [16]. Nevertheless, to the best of our knowledge, there is no report on the implication of lncRNA as an upstream regulator in nickel-induced lung tumorigenesis. In the present study, we discovered that nickel exposure led to *MEG3* downregulation through its promoter hypermethylation, and *MEG3* downregulation resulted in PHLPP1 transcriptional inhibition, consequently leading to HIF-1α protein translation elevation, and in turn promoting malignant transformation of human bronchial epithelial cells.

Results

Nickel-induced *MEG3* downregulation contributed to the malignant transformation of Beas2B cells

Although *MEG3* downregulation has been observed in various human tumors, including non-small cell lung cancer (NSCLC)[17], the impact of environmental carcinogens on *MEG3* expression and their potential contribution to lung tumorigenesis have never been explored. To test this, human bronchial epithelial cell line Beas2B cells were exposed to different doses of $NiCl_2$ over varying time periods, and *MEG3* expression was assessed by quantitative PCR. As shown in Figures 1A & 1B, exposure to $NiCl_2$ caused a time- and dose-dependent downregulation of *MEG3* expression in Beas2B cells. The human bronchial epithelial cell line BEP2D is an established clonal population of HPV-18-immortalized human bronchial epithelial cells, and provides another model to study the molecular pathogenesis of lung cancer[18]. In the present study, as shown in Figures 1C& D, downregulation of *MEG3* expression was also observed in BEP2D cells in a time- and dose-dependent fashion. These results demonstrate that nickel exposure results in attenuation of *MEG3* expression in human bronchial epithelial cells.

We next evaluated *MEG3* expression in lung tissues from patients with lung squamous cell carcinoma (SCC). *MEG3* expression in lung SCC was profoundly downregulated in comparison to those of the corresponding adjacent non-tumor lung tissues ($n=13$, $p<0.05$) (Figure 1E & Supplemental Table S1). It was noted that *MEG3* expression in adenocarcinoma was also inhibited ($n=17$, $p<0.05$) (Supplemental Figure S1 & Table S1). We made a comparison of the *MEG3* level in Beas2B and BEP2D cells with the normal lung tissue samples. There was no significant difference of the *MEG3* level between the normal lung tissues and Beas2B cells or BEP2D cells ($t=1.472$, $p=0.087$; $t=1.365$, $p=0.099$, respectively). Moreover, the *MEG3* levels in Beas2B or BEP2D cells with 0.5 mM nickel treatment for 6h also showed no significant difference in comparison to the lung cancer samples ($t=1.037$, $p=0.136$; $t=1.047$, $p=0.139$, respectively). Collectively, our results

demonstrate that *MEG3* downregulation was not only observed in nickel-exposed human bronchial epithelial cells, but also exhibited in human lung cancer tissues.

To determine whether *MEG3* downregulation plays a role in nickel-induced cell transformation, *MEG3* overexpression plasmid was stably transfected into Beas2B cells with G418 antibiotic selection. *MEG3* was overexpressed over 300-fold in stable transfectant Beas2B(MEG3) in comparison to the scramble control transfectant Beas2B(Vector) (Figure 1F). It is significant to note that ectopically expressed *MEG3* was not downregulated by nickel exposure, while endogenous *MEG3* was attenuated in Beas2B(Vector) cells due to nickel exposure (Figure 1G). We then repeatedly exposed the Beas2B(MEG3) and Beas2B(Vector) cells to nickel for 3 months, and the anchorage-independent growth capability of nickel-treated cells was evaluated in soft agar. As shown in Figures 1H & 1I, the *MEG3* overexpression led to significant inhibition of Beas2B cell transformation by nickel in comparison to the scramble control transfectant under the same experimental conditions, suggesting that *MEG3* provides an inhibitory effect on cell transformation of human bronchial epithelial cells induced by nickel exposure. To further test this notion, the short hairpin RNA (shRNA) knockdown endogenous *MEG3* expression was employed. As shown in Figure 1J, the stably expressed shMEG3 profoundly impaired *MEG3* expression in Beas2B cells. Stable knockdown of *MEG3* expression alone resulted in a remarkably spontaneous cell transformation of Beas2B cells, and also significantly promoted nickel-induced transformation of Beas2B cells (Figures 1K & 1L). The regulatory effect of *MEG3* on cell growth was also consistently observed in monolayer growth assay with above gain- or loss-expression of *MEG3* in Beas2B cell transfectants, including the parental Beas2B, Beas2B(vector), Beas2B(MEG3), Beas2B(nonsense), and Beas2B(shMEG3)(Supplemental Figure S2). Those results strongly demonstrate that *MEG3* downregulation contributes to malignant transformation of human bronchial epithelial cells due to nickel exposure.

MEG3 promoted HIF-1α protein translation following nickel exposure

Our previous studies have shown that nickel exposure elevates HIF-1α protein accumulation in various cells, and HIF-1α is involved in cell transformation in anchorage-independent growth assay[9]. As expected, nickel exposure accumulated HIF-1α protein in a time- and dose-dependent manner in Beas2B cells (Figures 2A & 2B). To evaluate whether *MEG3* is involved in nickel-induced HIF-1α protein accumulation, HIF-1α protein level in Beas2B(MEG3) was compared with that in Beas2B(Vector) cells following nickel exposure. As shown in Figure 2C, nickel-induced HIF-1α protein was barely observable in Beas2B(MEG3) following nickel exposure, whereas Beas2B(Vector) showed a marked induction of HIF-1α protein under the same experimental conditions. Moreover, stable knockdown of *MEG3* expression alone resulted in an increase in the basal level of HIF-1α protein expression, and also significantly promoted nickel-induced HIF-1α protein abundance (Figure 2D). Our results reveal that *MEG3* is an important player in the regulation of HIF-1α protein abundance in human bronchial epithelial cells following nickel exposure.

HIF-1α expression is well known for its regulation at the transcriptional and protein degradation levels due to hypoxia or the hypoxia mimetic agents[5]. However, our results from

RT-PCR showed no observable difference at *hif-1α* mRNA levels between Beas2B(MEG3) and Beas2B(Vector) cells following nickel exposure (Figure 2E), suggesting that *MEG3*-mediated HIF-1α abundance upon nickel exposure might occur at the post-transcriptional level. Following this, the HIF-1α protein degradation rate was then evaluated. As shown in Figure 2F, after treatment of cells with nickel plus the proteasome inhibitor MG132 for 6 h, the cell culture medium was replaced with the medium containing cycloheximide (CHX) to prevent *de novo* new protein synthesis, and both Beas2B(Vector) and Beas2B(MEG3) were used to determine HIF-1α protein degradation rates. The results showed that two stable transfectants have very similar HIF-1α protein degradation rates (Figure 2F), excluding *MEG3* regulates HIF-1α protein expression at the protein degradation level. This notion was consistently supported by the results obtained from the observation of HIF-1α protein degradation in both Beas2B(Vector) and Beas2B(MEG3) treated with dimethyloxaloylglycine (DMOG), an inhibitor of prolyl hydroxylase (PHD) (Figure 2G). Thus, we next determined the possibility of *MEG3* regulation of HIF-1α protein translation using [^{35}S]-labeled methionine and cysteine in pulse analysis. As shown in Figures 2H & 2I, the incorporation of [^{35}S]-labeled methionine and cysteine into newly synthesized HIF-1α protein was inhibited in Beas2B(MEG3) cells, although it was gradually increased along with the incubation time periods in both Beas2B(MEG3) and Beas2B(Vector) cells. Our results demonstrate that *MEG3* downregulation was crucial for HIF-1α protein translation following nickel exposure in human bronchial epithelial cells.

Akt/p70S6K/S6 pathway played an important role in *MEG3* regulation of HIF-lα protein translation

Ribosome biogenesis is a fundamental process that provides cells with the molecular factories for cellular protein production[19]. The ribosome is a complex molecular machine that is composed of a small 40S and a large 60S subunit. Phosphorylation at Ser235/236 of the 40S ribosomal protein S6 plays an important role in the regulation of protein translation[20]. Thus, the phosphorylation at Ser235/236 of S6 was evaluated following nickel exposure in Beas2B cells. As shown in Figure 3A, nickel exposure led to an increase in S6 phosphorylations at Ser235/236 in the early time phase (1–6 h after exposure). To examine whether *MEG3* was implicated in modulation of S6 phosphorylations at Ser235/236 following nickel exposure, we compared the S6 phosphorylation at Ser235/236 between Beas2B(MEG3) cells and Beas2B(Vector) cells. The results indicated that S6 phosphorylations at Ser235/236 was completely inhibited in Beas2B(MEG3) cells in comparison to the Beas2B(Vector) cells (Figure 3B). The findings were further validated in *MEG3* knockdown transfectants, which showed an increase in S6 phosphorylation at Ser235/236 as compared with Beas2B(Nonsense) cells following nickel exposure (Figure 3C). The mammalian target rapamycin (mTOR) is the upstream kinase mediating S6 phosphorylations at Ser235/236[21]. To test the role of S6 phosphorylation in HIF-1α protein translation, rapamycin, a specific inhibitor of mTOR, was employed. As shown in Figure 3D, pretreatment of cells with rapamycin blocked S6 phosphorylation at Ser235/236 and HIF-1α protein accumulation following nickel exposure. Moreover, knockdown of S6 expression by shRNA also inhibited HIF-1α accumulation following nickel exposure (Figure 3E), strongly supporting our notion that *MEG3* inhibited HIF-1α translation *via* attenuation of the S6 phosphorylation at Ser235/236.

Our previous studies have demonstrated that nickel exposure leads to activation of phosphatidylinositol 3-kinase (PI-3K), Akt, and p70S6 kinase (p70S6k)[7]. Akt activation has been found to be implicated in ribosomal S6 kinase (S6K1)/S6-dependent p53 protein translation in arsenite-treated cells[22]. Thus, Akt phosphorylation at Ser473 was evaluated in both *MEG3* overexpressed and knockdown Beas2B cells in comparison to the corresponding vector control transfectants following nickel exposure. The results showed that the increase of Akt phosphorylation at Ser473 was consistent with the increase of S6 phosphorylation at Ser235/236 following nickel exposure in Beas2B cells (Figure 3A). Moreover, the increase of Akt phosphorylation at Ser473 by nickel was completely abolished by ectopic overexpression of *MEG3* and remarkably enhanced by knockdown of *MEG3* (Figures 3B & 3C). To test whether Akt activation mediated S6 phosphorylation at Ser235/236 and HIF-1α protein translation following nickel exposure, we transiently transfected the dominant-negative mutant Akt (DN-Akt, AktT308A/S473A) into Beas2B(shMEG3) cells, and the transient transfectant Beas2B(shMEG3/DN-Akt) and its vector control transfectant Beas2B(shMEG3/Vector) were evaluated. Overexpression of DN-Akt blocked nickel-induced Akt phosphorylation at Ser473, p70S6K phosphorylation at Thr389, and S6 phosphorylation at Ser235/236, as well as HIF-1α protein accumulation following nickel exposure (Figure 3F). Our results strongly indicate that the Akt/p70S6k/S6 pathway plays an important role in *MEG3* regulation of HIF-1α protein translation.

PHLPP1 was responsible for *MEG3*-mediated inhibition of Akt/p70S6K/S6 pathway activation

The phosphatase and tensin homolog (PTEN) is a tumor suppressor that negatively regulates the PI-3K/Akt pathway by dephosphorylation of the lipid second message, phosphatidylinositol-3,4,5-trisphosphate, a product of phosphatidylinositol 3-kinase (PI-3K), by which PTEN inhibits Akt activation [23]. PH domain leucine-rich repeat protein phosphatase (PHLPP) is a protein phosphatase, that is comprised of PHLPP1 and PHLPP2 two members, which are able to specifically dephosphorylate the hydrophobic motif of Akt (Ser473 in Akt)[24]. Protein phosphatase 2A (PP2A) has also been reported to be a negative regulator of the Akt pathway [25]. To identify the downstream effector of *MEG3* that mediated the Akt/p70S6K/S6 pathway activation, we compared the expression of PTEN, PHLPP1, PHLPP2, and PP2A in Beas2B(MEG3) vs. Beas2B(Vector) and Beas2B(shMEG3) vs. Beas2B(Nonsense) cells following nickel exposure. As shown in Figure 4A, overexpression of *MEG3* specifically reversed nickel downregulation of PHLPP1 protein expression in comparison to Beas2B(Vector). Although knockdown of *MEG3* also changed the protein levels of p-PTEN, p-PP2A, PP2A-B, and PHLPP2, but those change could not be reversed by overexpression of *MEG3* in Beas2B(MEG3) cells (Figures 4A & 4B). Therefore, we anticipate that PHLPP1 might be the potential target of *MEG3* in Beas2B cells. It is highly significant to note that PHLPP1 downregulation was also observed in lung cancer tissues (Figures 4C & 4D). Moreover, there was a highly significant positive correlation between *MEG3* and PHLPP1 (ρ=0.846, P=0.000) (Supplemental Figure S3A). These results reveal that PHLPP1 might be an *MEG3* downstream phosphatase responsible for dephosphorylation of Akt following nickel exposure. To this end, we used shRNA to knockdown of PHLPP1 in Beas2B(MEG3) cells. As shown in Figure 4E, knockdown of PHLPP1 led to marked increases in the phosphorylation of Akt at Ser473, p70S6K at

Thr389 and S6 at Ser235/236, as well as induction of HIF-1α protein. It was noted that *MEG3* expression level in constitutive stable Beas2B(MEG3) transfectants is over 300-fold. To avoid constitutive over 300-fold *MEG3* expression impacting on intrinsic cell function, we constructed an inducible expression plasmid pTRE-MEG3, which was also stably transfected into Beas2B cells. The stable transfectant, Beas2B(pTRE-MEG3), showed around 30-fold *MEG3* expression upon treatment with 10 μg/ml Dox in comparison to the vector control transfectants under the same experimental conditions (Supplemental Figure S4). The effect of *MEG3* on the expression of HIF-1α and PHLPP1, as well as the phosphorylation of c-Jun at Ser73, Akt at Ser473, p70 S6K at Thr389 and S6 at Ser235/236, has been validated in the inducible *MEG3* stable transfectants in the absence or presence of Dox (Supplemental Figure S5). Collectively, our results demonstrate that PHLPP1 is an *MEG3* downstream phosphatase in regulation of phosphorylations of Akt at Ser473, p70S6K at Thr389, and S6 at Ser235/236, as well as expression of HIF-1α protein following nickel exposure.

MEG3 regulated PHLPP1 transcription *via* interaction with transcription factor c-Jun

To evaluate the molecular mechanisms underlying *MEG3* downregulation of PHLPP1 expression, we detected the *phlpp1* mRNA levels in Beas2B(MEG3) vs. Beas2B(Vector) and Beas2B(shMEG3) vs. Beas2B(Nonsense) cells following nickel exposure. As shown in Figure 5A, overexpression of *MEG3* was able to increase the basal level of *phlpp1* mRNA expression and that it also brought *phlpp1* mRNA in nickel-treated Beas2B(MEG3) up to the basal level observed in Beas2B(Vector) cells. Consistently, knockdown of *MEG3* resulted in a remarkably reducing the *phlpp1* mRNA expression (Figure 5B). Moreover, overexpression of *MEG3* also increased the promoter transcriptional activity (Figure 5C), indicating *MEG3* upregulates PHLPP1 expression at the transcriptional level. To test the possibility of transcriptional regulation, bioinformatics software was used to analyze the potential transcription factor binding sites in *phlpp1* promoter region. The results showed that there were multiple potential transcription factor binding sites, including c-Jun, Jun B, c-Myc, JunD, Sp1, and Ets-1, in the *phlpp1* promoter region (Figure 5D). Thus, we then focused on identification of the potential transcription factors contribution to *phlpp1* mRNA expression by comparing the effect of *MEG3* on the transcription factors expression and their activation following nickel exposure. As the results shown in Figure 5E, overexpression of *MEG3* inhibited expression of c-Jun and c-Myc, while it did not show a remarkable effect on other transcription factors, including Jun B, Jun D, Sp1, or Ets-1. The effect of *MEG3* on the expression of c-Jun and c-Myc was further validated in Beas2B(shMEG3) cells(Figure 5F). These results are also consistent with our most recently findings that nickel exposure leads to a marked nuclear translocation of c-Jun and c-Myc[26]. Therefore, we proposed that c-Jun and c-Myc might be the transcription factors for negative regulation of *phlpp1* promoter transactivation through direct binding. To test this possibility, a series of *phlpp1* promoter-driven luciferase reporters containing incrementally deleted sequences in the −1946/−207 region (numbers relative to the transcription start site), as indicated in Figure 5G, were stably transfected into Beas2B(pTRE-MEG3) and Beas2B(Vector) cells. The results showed that the promoter transcriptional activity was completely attenuated in the transfectant with the −417/−207 luciferase reporter in comparison to the transactivation observed in the transfectants with other luciferase reporters (Figure 5H), suggesting that the transcription

factor binding site at −555 (c-Jun) is the critical one responsible for *phlpp1* transcription. To test this possibility, c-Jun was specifically knockdown in Beas2B(shMEG3) cells, as expected, knockdown of c-Jun promoted *PHLPP1phlpp1* mRNA and protein expression (Figures 5I & 5J). To provide experimental evidence showing c-Jun directly binding to *phlpp1* promoter, ChIP assay was performed. As shown in Figure 5K, the −808/−417 region of *phlpp1* promoter that contains tentative c-Jun binding site was specifically presented in the immunoprecipitated complex using anti-c-Jun antibody in ChIP assay. To demonstrate the inhibition of c-Jun transactivation activity by its interaction with *MEG3*, an RNA immunoprecipitation assay was further performed. The results indicated that the immunoprecipitated complex pulled down by anti-c-Jun from Beas2B(MEG3) cells contained *MEG3* transcript (Figure 5L), strongly demonstrating that *MEG3* positively regulates *phlpp1* mRNA transcription by interacting with c-Jun and disrupting c-Jun binding to *phlpp1* promoter.

DNMT3b-mediated promoter hypermethylation contributed to *MEG3* downregulation and HIF-1α protein upregulation following nickel exposure

It has been reported that the *MEG3* promoter hypermethylation is an important mechanism associated with the loss of *MEG3* expression in clinically nonfunctioning pituitary tumors[27]. To investigate whether the downregulation of *MEG3* expression in nickel exposure is due to promoter hypermethylation, we treated Beas2B cells with NiCl2 over various time periods, and assessed *MEG3* promoter methylation at the differentially methylated region (DMR) using Methylation-Specific PCR (MS-PCR). The extent of the DMR of human *MEG3* was shown to span approximately 4 kb of genomic sequence that encompasses the putative promoter region and includes two consensus CTCF (CCCTC binding factor) binding sites that also exhibit differential methylation[28]. In the present study, we referenced the studies from Murphy et al. [28], which have designed two independent primer sets to amplify the methylated and unmethylated DMR. The region analyzed by MS-PCR is from nt 64,450 to nt 66,150 of accession no. AL117190, spans ~1,700 *bp*, which correspond to sequences within the CpG-rich regions upstream of *MEG3*. As shown in Figure 6A, nickel treatment caused a time-dependent upregulation of methylated DNA (M), produced a 160-bp band, accompanied with the downregulation of unmethylated DNA (U), produced a 120-bp band, in Beas2B cells. To further explore the role of promoter hypermethylation in *MEG3* downregulation, the DNA methyltransferase inhibitor, 5-aza-2'-deoxycytidine, was used to inhibit DNA methylation in genomic DNA. The results showed that the treatment of cells with 5-aza-2'-deoxycytidine inhibited nickel-induced methylation of *MEG3* promoter (Figure 6B) and reversed the inhibition of nickel-induced *MEG3* downregulation that was observed in Beas2B cells treated with nickel only (Figure 6C). Consistently, 5-aza-2'-deoxycytidine treatment also attenuated HIF-1α protein abundance due to nickel exposure in Beas2B cells (Figure 6D). These results reveal that nickel exposure led to *MEG3* promoter hypermethylation contributes to HIF-1α protein expression in human bronchial epithelial cells.

DNA methyltransferases (DNMTs) are enzymes that are responsible for the transfer of a methyl group from the universal methyl donor, S-adenosyl-L-methionine (SAM), to the 5-position of cytosine residues in DNA[29]. To investigate the effect of DNMTs on the

hypermethylation of *MEG3* differentially methylated regions (DMRs), we first evaluated the potential effect of short and long-term nickel exposure on the mRNA expression of DNMTs, including *dnmt1, dnmt3a* and *dnmt3b*. The results indicated that nickel exposure specifically induced mRNA expression of *dnmt3b*, but not *dnmt1* and *dnmt3a*, following treatment of Beas2B cells with nickel for either 12 hours or 6 months (Figures 6E & 6F). The upregulation of DNMT3b protein has also been observed in human lung cancer tissues (Figures 6G & 6H) and nickel-exposed Beas2B cells (Figures 6I & 6J). Moreover, data analyses showed a highly negative correlation between DNMT3b expression and *MEG3* level ($\rho=-0.725$, $P=0.005$), whereas no significant correlation was observed between PHLPP1 and DNMT3b ($\rho=-0.523$, $P= 0.067$) (Supplemental Figures S3B & S3C), revealing that DNMT3b might be directly regulating *MEG3* expression, but not PHLPP1, following nickel exposure. To explore this relationship between DNMT3b and *MEG3*, specific sgRNA targeting DNMT3b was used to stably knockout *dnmt3b* in Beas2B cells. As shown in Figures 6K & 6L, DNMT3b knockout reversed nickel-induced *MEG3* downregulation, increased in PHLPP1 expression and blocked Akt phosphorylation at Ser473, p70S6K phosphorylation at Thr389, S6 phosphorylation at Ser235/236, and HIF-1α protein induction in Beas2B cells due to nickel exposure. Consistently, DNMT3b knockout also abolished malignant transformation of human bronchial epithelial cells due to nickel exposure (Figures 6M& 6N). Taken together, our results strongly demonstrate that DNMT3b upregulation contributes to nickel-induced *MEG3* promoter hypermethylation, which leads to inhibition of *MEG3* expression, consequently resulting in c-Jun activation, *phlpp1* transcriptional reduction, and in turn promoting HIF-1α protein translation *via* activation of the Akt/p70S6K/S6 axis in Beas2B cells as summarized in Figure 6O.

Discussion

MEG3, as a tumor suppressor, is expressed in multiple normal tissues of human internal organs[13]. The loss of *MEG3* expression has been thought to be a primary feature of human cancers, such as liver cancer[30], gastric cancer[31], colorectal cancer[32], glioma[33], cervical cancer[34], bladder cancer[35], prostate cancer[36], and lung cancer[17]. However, whether *MEG3* is reducible upon environmental carcinogen exposure, what are the upstream regulators that lead to *MEG3* expression and the downstream effectors mediating tumor suppressive function, as well as how *MEG3* contributes to the tumorigenicity of environmental carcinogen has never been explored. In the present study, we found that nickel was able to inhibit *MEG3* expression in human bronchial epithelial cells. Since squamous cell carcinoma is the major histological type in lung cancers of nickel-refinery workers, we have compared *MEG3* expression in lung cancer tissues with their adjacent non-tumor lung tissues. The results consistently show the downregulation of *MEG3* expression in squamous cell carcinomas. We have further demonstrated that downregulation of *MEG3* is an important player for nickel-induced the transformation of human bronchial epithelial cells. Thus, our present studies not only, for the first time, discover the downregulation of *MEG3* expression due to nickel exposure, they also demonstrate the contribution of *MEG3* downregulation to malignant transformation of human bronchial epithelial cell following nickel exposure.

Hypoxia inducible factor-1 (HIF-1) is a master transcription factor that is critical for the regulation of the hypoxic response in eukaryotic cells. Deregulation of HIF-1 activity is mainly associated with the expression of HIF-1α subunit, a key regulatory subunit responsible for HIF-1 transcriptional function[37]. Oxygen-dependent hydroxylation of the HIF-1α subunit by prolyl hydroxylase domain (PHD) proteins signals their polyubiquitination and proteasomal degradation, and plays a critical role in regulating HIF-1α abundance and oxygen homeostasis[38]. Some environmental factors, including nickel, can inhibit PHD activity and cause HIF-1α stabilization[39]. Moreover, our published studies show that HIF-1α mRNA and protein stabilization can also be regulated by JNK2[10] and JNK1[9], respectively. However, translational regulation of HIF-1α, particularly under environmental carcinogen such as nickel, has never been explored. Our current studies demonstrate that *MEG3* play a crucial role in nickel-induced HIF-1α protein translation. We showed that overexpression of *MEG3* inhibited HIF-1α protein abundance, while knockdown of *MEG3* increased HIF-1α protein expression by nickel exposure. In contrast to the protein abundance, HIF-1α mRNA levels and protein degradation rates were comparable between Beas2B(MEG3) vs. Beas2B(Vector) following nickel exposure, excluding the possibility that *MEG3* regulates HIF-1α abundance at levels of transcription, mRNA stability or protein degradation although they are implicated in HIF-1α protein induction by nickel. The results obtained using [35S]-labeled methionine and cysteine for new protein synthesis clearly reveal that *MEG3* is able to inhibit HIF-1α protein translation. Ribosomal protein S6 is a well-known mediator of protein translation, phosphorylation of S6 promotes the recruitment of the 40S ribosome to the mRNA and therefore has a paramount effect on protein translation[40]. Our results indicated that overexpression of *MEG3* inhibited nickel-induced S6 phosphorylation at Ser235/Ser236, whereas knockdown of *MEG3* significantly increased S6 phosphorylation at Ser235/Ser236. We further found that *MEG3* downregulation resulted in S6 activation, and in turn directly promoting protein translation as demonstrated by the results obtained from comparison of S6 phosphorylation at Ser235/Ser236 in Beas2B(MEG3) vs. Beas2B(Vector) and Beas2B(shMEG3) vs. Beas2B(Nonsense), and utilization of mTOR inhibitor rapamycin and the shRNA specific targeting S6. By tracking the upstream pathways responsible for phosphorylation of S6, we defined *MEG3* inhibition of Akt phosphorylation at Ser473, which is an upstream regulator directly mediating p70S6K/S6 phosphorylation and activation. Precise control of the balance of protein phosphorylation and dephosphorylation that is catalyzed by protein kinases and phosphatases is essential for cellular homeostasis. PTEN[41], PP2A[25] and PHLPP[24] are three ubiquitously expressed phosphatases that have been reported to dephosphorylate many critical cellular molecules, such as Akt. Our further mechanistic elucidation indicates that PHLPP1, but not PP2A and PTEN, is an *MEG3* downstream effector responsible for its inhibition of Akt phosphorylation and HIF-1α protein translation upon nickel exposure. Those results may be extent to human, since we found a strong positive correlation between *MEG3* and PHLPP1 expression in lung cancer tissues.

c-Jun has been reported to play an important role in regulation of cellular proliferation, transformation and death[42] and it promotes cellular survival by negatively regulating the expression of the tumor-suppressor PTEN, resulting in the concomitant activation of the Akt survival pathway[43]. Here we show that *MEG3* regulates *phlpp1* transcription through its

direct interaction with the c-Jun and inhibition of c-Jun activity, while c-Jun is a negative transcription factor for *phlpp1* promoter transcription. We found that c-Jun negatively regulates *phlpp1* transcription by binding directly to the *phppp1* promoter, and that *MEG3* is able to bind to the c-Jun transcription factor and decrease c-Jun activity in the inhibition of *phlpp1* promoter transcription. Thus, a highly specific and stable triplex structure formed by *MEG3*, together with the c-Jun and the *phlpp1* promoter, results in *MEG3* promotion of *phlpp1* transcription.

Silencing of genes by aberrant promoter hypermethylation is one of the mechanisms leading to tumor suppressor downregulation and cancer initiation and progression[44]. It has been reported that hypermethylation of the *MEG3* regulatory region has also been associated with the loss of *MEG3* expression in human tumors cell lines, such as pituitary tumors[27], gliomas[45] and hepatoma[46]. In the present study, we found that environmental carcinogen nickel resulted in the hypermethylation of *MEG3* regulatory region in normal human bronchial epithelial cells, and that treatment of cells with DNA methylation inhibitor 5-aza-2-deoxycytidine (5-Aza) increased in *MEG3* expression, strongly indicating that the promoter hypermethylation mediates downregulation of *MEG3* transcription due to nickel exposure. Methylation of mammalian genomic DNA is catalyzed by DNMTs[47]. In mammals, there are 3 major DNMTs: DNMT1, DNMT3a, and DNMT3b. DNMT1 is a maintenance DNMT, while DNMT3a and 3b are *de novo* DNMTs[48]. Our further elucidation shows that nickel exposure upregulated DNMT3b expression, and that knockout of DNMT3b promoted *MEG3* and PHLPP1 expression, accompanied by inhibition of Akt/p70/S6 pathway activation, HIF-1α accumulation, and malignant transformation of Beas2B cells. Collectively, our studies demonstrate the crucial role of DNMT3b induction in the mediation of promoter hypermethylation and downregulation of *MEG3*, as well as their contribution to nickel-induced lung tumorigenicity. Those results may also be extent to human, since we found a strong negative correlation between DNMT3b and *MEG3* expression in lung cancer tissues.

In summary, our results define a novel effect of nickel on *MEG3* reduction and the upstream epigenetic regulator DNMT3b leading to this reduction, as well as the mechanisms underlying its interaction with downstream effector c-Jun, consequently resulting in attenuation of PHLPP1 expression, Akt/p70S60K/S6 activation, HIF-1α protein translation as well as malignant transformation of human bronchial epithelial cells. These findings demonstrate the association and function of *MEG3* in nickel-induced lung tumorigenesis and provide novel insights into understanding of the multiple levels of HIF-1α protein regulation in nickel responses.

Materials and Methods

Cell lines, Plasmids, Antibodies, and Other reagents

These details are described in Supplemental Information.

Patients and Tumor Sample Preparation

Thirteen pairs of lung squamous cell carcinoma, seventeen pairs of lung adenocarcinoma and adjacent non-tumor tissue specimens were obtained from surgical specimens at The First Affiliated Hospital of Wenzhou Medical University (Wenzhou, China) after informed consent. Lung squamous cell carcinoma was diagnosed histopathologically and clinical characteristics of the patients included in this study were presented in Supplementary materials. Adjacent non-tumor tissue specimens were taken from a standard distance (3 cm) from the margin of resected neoplastic tissues of patients with tumors who ensured surgical lung ablation. All these specimens were snap-frozen in liquid nitrogen after excision. This study was compliant with the Declaration of Helsinki Guidelines and was approved by the Medical Ethics Committee of Wenzhou Medical University. Informed consent was obtained from each participant and the procedures were carried out in accordance with the approved guidelines.

Cell Transformation and Anchorage-independent Growth Assay

Cell transformation was performed using anchorage-independent growth in soft agar as described in our previous publication[9].

Luciferase Reporter Assay

Luciferase reporter assays were performed as described in our previous publication[49].

[^{35}S]-labeled Methionine-Cysteine Pulse Assay

The [^{35}S]-labeled methionine-cysteine pulse assay was performed as described in our previous publication[9]. [^{35}S]-labeled HIF-1α protein was detected with the Phosphor Imager (Molecular Dynamics, Kent City, MI, USA) and analyzed by calculating the integrated optical density per band area (IOD/area) using the Alpha Innotech SP image system (Alpha Innotech Corporation, USA).

DNA Extraction, Bisulfite DNA Modification, and Methylation-Specific PCR

Genomic DNA from Beas2B cells was extracted using DNeasy Blood & Tissue Kit (Qiagen, Gaithersburg, MD, USA) according to the manufacturer's guidelines. Sodium bisulfite modification of DNA and subsequent purification was performed according to the manufacturer's guidelines for sodium bisulfite conversion of unmethylated cytosine in DNA using EpiTect Bisulfite kit (Qiagen, Gaithersburg, MD, USA).

Bisulfite-treated genomic DNA was subjected to an optimized methylation-specific PCR, and was performed as previously described[28].

Semiquantitative and quantitative RT-PCR

Semiquantitative or quantitative RT-PCR was performed to examine the expression level of mRNA and lncRNA *MEG3*, respectively, as previously described[49]. The primers used in this study are listed in Supplemental Table S2.

Immunohistochemistry (IHC) Staining

For immunohistochemistry staining, we respectively used antibodies specific against PHLPP1 and DNMT3b, and the protein expression levels were analyzed as previously described[50].

Western Blotting

Western Blotting was performed as previously described[10].

Chromatin Immunoprecipitation (ChIP)

Chromatin immunoprecipitation (ChIP) assays were performed using the EZ-ChIP chromatin immunoprecipitation kit (Millipore, Billerica, MA, USA) according to the manufacturer's guidelines. Immunoselections of cross-linked protein-DNA were performed using anti-c-Jun antibody together agarose beads A/G, at 4 °C for overnight. The anti-rabbit IgG was used as a negative control. The purified DNAs were analyzed by PCR, the forward and reverse primers were: 5'- GGT GTG ACG GGT GTG TAT CT −3' and 5'- GTA TTT TAC CCG CAC TCC AGC −3' for human *phlpp1* promoter.

RNA Immunoprecipitation (RIP)

RNA Immunoprecipitation was performed as previously described[10]. The RNAs in the buffer were extracted by TriZol reagent. qPCR was performed to detect the *MEG3* presented in the immune-complex.

Statistical Analysis

All of the statistical analyses were performed by SPSS 17.0 software (SPSS Inc., Chicago, IL, USA). The student's *t*-test was used to determine the significance of differences between two groups. The *MEG3* expression in lung cancer tissues was compared with that of the corresponding adjacent non-tumor lung tissues using the paired samples *t*-test. *P* value with less than 0.05 was considered to be statistically significant.

Acknowledgments

We greatly appreciated Dr. Shau-Ping Lin (Institute of Biotechnology, National Taiwan University, Taipei, Taiwan) for his generous gifts about shRNA constructs against *MEG3* and control vector. This work was supported partially by grants from NIH/NCI CA112557, CA165980 and CA177665, NIH/NIEHS ES000260, National Natural Science Foundation of China (81441090, 81229002, 81372946, 81673141 and 81371730), the Specialized Research Fund for the Doctoral Program of Higher Education (20133420110001), the Key Project of Science and Technology Innovation Team of Zhejiang Province (2013TD10), and the Grant for Scientific Research of BSKY (XJ201418) from Anhui Medical University. We also thanks Ms. Nedda Tichi for her critically reading of the manuscript.

References

1. Siegel RL, Miller KD, Jemal A. Cancer Statistics, 2016. Ca-Cancer J Clin. 2016; 66:7–30. [PubMed: 26742998]
2. Field RW, Withers BL. Occupational and environmental causes of lung cancer. Clin Chest Med. 2012; 33:681–703. [PubMed: 23153609]
3. Kasprzak KS, Sunderman FW Jr, Salnikow K. Nickel carcinogenesis. Mutat Res. 2003; 533:67–97. [PubMed: 14643413]

4. Lu H, Shi X, Costa M, Huang C. Carcinogenic effect of nickel compounds. Mol Cell Biochem. 2005; 279:45–67. [PubMed: 16283514]
5. Ke Q, Costa M. Hypoxia-inducible factor-1 (HIF-1). Mol Pharmacol. 2006; 70:1469–1480. [PubMed: 16887934]
6. Lee JW, Bae SH, Jeong JW, Kim SH, Kim KW. Hypoxia-inducible factor (HIF-1)alpha: its protein stability and biological functions. Exp Mol Med. 2004; 36:1–12. [PubMed: 15031665]
7. Li J, Davidson G, Huang Y, Jiang BH, Shi X, Costa M, et al. Nickel compounds act through phosphatidylinositol-3-kinase/Akt-dependent, p70(S6k)-independent pathway to induce hypoxia inducible factor transactivation and Cap43 expression in mouse epidermal Cl41 cells. Cancer research. 2004; 64:94–101. [PubMed: 14729612]
8. Ouyang W, Zhang D, Li J, Verma UN, Costa M, Huang C. Soluble and insoluble nickel compounds exert a differential inhibitory effect on cell growth through IKKalpha-dependent cyclin D1 down-regulation. J Cell Physiol. 2009; 218:205–214. [PubMed: 18792914]
9. Zhang D, Li J, Costa M, Gao J, Huang C. JNK1 mediates degradation HIF-1alpha by a VHL-independent mechanism that involves the chaperones Hsp90/Hsp70. Cancer research. 2010; 70:813–823. [PubMed: 20068160]
10. Zhang D, Li J, Zhang M, Gao G, Zuo Z, Yu Y, et al. The requirement of c-Jun N-terminal kinase 2 in regulation of hypoxia-inducing factor-1alpha mRNA stability. The Journal of biological chemistry. 2012; 287:34361–34371. [PubMed: 22910906]
11. Esteller M. Non-coding RNAs in human disease. Nat Rev Genet. 2011; 12:861–874. [PubMed: 22094949]
12. Miyoshi N, Wagatsuma H, Wakana S, Shiroishi T, Nomura M, Aisaka K, et al. Identification of an imprinted gene, Meg3/Gtl2 and its human homologue MEG3, first mapped on mouse distal chromosome 12 and human chromosome 14q. Genes Cells. 2000; 5:211–220. [PubMed: 10759892]
13. Zhou Y, Zhang X, Klibanski A. MEG3 noncoding RNA: a tumor suppressor. J Mol Endocrinol. 2012; 48:R45–R53. [PubMed: 22393162]
14. Benetatos L, Vartholomatos G, Hatzimichael E. MEG3 imprinted gene contribution in tumorigenesis. Int J Cancer. 2011; 129:773–779. [PubMed: 21400503]
15. Salnikow K, Zhitkovich A. Genetic and epigenetic mechanisms in metal carcinogenesis and cocarcinogenesis: nickel, arsenic, and chromium. Chem Res Toxicol. 2008; 21:28–44. [PubMed: 17970581]
16. Hou L, Zhang X, Wang D, Baccarelli A. Environmental chemical exposures and human epigenetics. Int J Epidemiol. 2012; 41:79–105. [PubMed: 22253299]
17. Lu KH, Li W, Liu XH, Sun M, Zhang ML, Wu WQ, et al. Long non-coding RNA MEG3 inhibits NSCLC cells proliferation and induces apoptosis by affecting p53 expression. BMC Cancer. 2013; 13:461. [PubMed: 24098911]
18. Willey JC, Broussoud A, Sleemi A, Bennett WP, Cerutti P, Harris CC. Immortalization of normal human bronchial epithelial cells by human papillomaviruses 16 or 18. Cancer research. 1991; 51:5370–5377. [PubMed: 1717149]
19. Kressler D, Hurt E, Bassler J. Driving ribosome assembly. Biochim Biophys Acta. 2010; 1803:673–683. [PubMed: 19879902]
20. Ruvinsky I, Sharon N, Lerer T, Cohen H, Stolovich-Rain M, Nir T, et al. Ribosomal protein S6 phosphorylation is a determinant of cell size and glucose homeostasis. Genes Dev. 2005; 19:2199–2211. [PubMed: 16166381]
21. Shimobayashi M, Hall MN. Making new contacts: the mTOR network in metabolism and signalling crosstalk. Nat Rev Mol Cell Biol. 2014; 15:155–162. [PubMed: 24556838]
22. Yu Y, Zhang D, Huang H, Li J, Zhang M, Wan Y, et al. NF-kappaB1 p50 promotes p53 protein translation through miR-190 downregulation of PHLPP1. Oncogene. 2014; 33:996–1005. [PubMed: 23396362]
23. Wang J, Ouyang W, Li J, Wei L, Ma Q, Zhang Z, et al. Loss of tumor suppressor p53 decreases PTEN expression and enhances signaling pathways leading to activation of activator protein 1 and nuclear factor kappaB induced by UV radiation. Cancer research. 2005; 65:6601–6611. [PubMed: 16061640]

24. Newton AC, Trotman LC. Turning off AKT: PHLPP as a drug target. Annu Rev Pharmacol Toxicol. 2014; 54:537–558. [PubMed: 24392697]
25. Seshacharyulu P, Pandey P, Datta K, Batra SK. Phosphatase: PP2A structural importance, regulation and its aberrant expression in cancer. Cancer Lett. 2013; 335:9–18. [PubMed: 23454242]
26. Huang H, Zhu J, Li Y, Zhang L, Gu J, Xie Q, et al. Upregulation of SQSTM1/p62 contributes to nickel-induced malignant transformation of human bronchial epithelial cells. Autophagy. 2016; 12:1687–1703. [PubMed: 27467530]
27. Zhao J, Dahle D, Zhou Y, Zhang X, Klibanski A. Hypermethylation of the promoter region is associated with the loss of MEG3 gene expression in human pituitary tumors. J Clin Endocrinol Metab. 2005; 90:2179–2186. [PubMed: 15644399]
28. Murphy SK, Wylie AA, Coveler KJ, Cotter PD, Papenhausen PR, Sutton VR, et al. Epigenetic detection of human chromosome 14 uniparental disomy. Human mutation. 2003; 22:92–97. [PubMed: 12815599]
29. Jin B, Robertson KD. DNA methyltransferases, DNA damage repair, and cancer. Adv Exp Med Biol. 2013; 754:3–29. [PubMed: 22956494]
30. Anwar SL, Krech T, Hasemeier B, Schipper E, Schweitzer N, Vogel A, et al. Loss of imprinting and allelic switching at the DLK1-MEG3 locus in human hepatocellular carcinoma. PLoS One. 2012; 7:e49462. [PubMed: 23145177]
31. Sun M, Xia R, Jin F, Xu T, Liu Z, De W, et al. Downregulated long noncoding RNA MEG3 is associated with poor prognosis and promotes cell proliferation in gastric cancer. Tumour Biol. 2014; 35:1065–1073. [PubMed: 24006224]
32. Yin DD, Liu ZJ, Zhang E, Kong R, Zhang ZH, Guo RH. Decreased expression of long noncoding RNA MEG3 affects cell proliferation and predicts a poor prognosis in patients with colorectal cancer. Tumour Biol. 2015; 36:4851–4859. [PubMed: 25636452]
33. Wang P, Ren Z, Sun P. Overexpression of the long non-coding RNA MEG3 impairs in vitro glioma cell proliferation. J Cell Biochem. 2012; 113:1868–1874. [PubMed: 22234798]
34. Zhang J, Yao T, Wang Y, Yu J, Liu Y, Lin Z. Long noncoding RNA MEG3 is downregulated in cervical cancer and affects cell proliferation and apoptosis by regulating miR-21. Cancer Biol Ther. 2016; 17:104–113. [PubMed: 26574780]
35. Ying L, Huang Y, Chen H, Wang Y, Xia L, Chen Y, et al. Downregulated MEG3 activates autophagy and increases cell proliferation in bladder cancer. Mol Biosyst. 2013; 9:407–411. [PubMed: 23295831]
36. Luo G, Wang M, Wu X, Tao D, Xiao X, Wang L, et al. Long Non-Coding RNA MEG3 Inhibits Cell Proliferation and Induces Apoptosis in Prostate Cancer. Cell Physiol Biochem. 2015; 37:2209–2220. [PubMed: 26610246]
37. Weidemann A, Johnson RS. Biology of HIF-1alpha. Cell Death Differ. 2008; 15:621–627. [PubMed: 18259201]
38. Fong GH, Takeda K. Role and regulation of prolyl hydroxylase domain proteins. Cell Death Differ. 2008; 15:635–641. [PubMed: 18259202]
39. Salnikow K, Donald SP, Bruick RK, Zhitkovich A, Phang JM, Kasprzak KS. Depletion of intracellular ascorbate by the carcinogenic metals nickel and cobalt results in the induction of hypoxic stress. The Journal of biological chemistry. 2004; 279:40337–40344. [PubMed: 15271983]
40. Magnuson B, Ekim B, Fingar DC. Regulation and function of ribosomal protein S6 kinase (S6K) within mTOR signalling networks. Biochem J. 2012; 441:1–21. [PubMed: 22168436]
41. Georgescu MM. PTEN Tumor Suppressor Network in PI3K-Akt Pathway Control. Genes Cancer. 2010; 1:1170–1177. [PubMed: 21779440]
42. Shaulian E, Karin M. AP-1 as a regulator of cell life and death. Nat Cell Biol. 2002; 4:E131–E136. [PubMed: 11988758]
43. Hettinger K, Vikhanskaya F, Poh MK, Lee MK, de Belle I, Zhang JT, et al. c-Jun promotes cellular survival by suppression of PTEN. Cell Death Differ. 2007; 14:218–229. [PubMed: 16676006]
44. Belinsky SA. Gene-promoter hypermethylation as a biomarker in lung cancer. Nat Rev Cancer. 2004; 4:707–717. [PubMed: 15343277]

45. Li J, Bian EB, He XJ, Ma CC, Zong G, Wang HL, et al. Epigenetic repression of long non-coding RNA MEG3 mediated by DNMT1 represses the p53 pathway in gliomas. Int J Oncol. 2016; 48:723–733. [PubMed: 26676363]

46. Liu LX, Deng W, Zhou XT, Chen RP, Xiang MQ, Guo YT, et al. The mechanism of adenosine-mediated activation of lncRNA MEG3 and its antitumor effects in human hepatoma cells. Int J Oncol. 2016; 48:421–429. [PubMed: 26647875]

47. Okano M, Bell DW, Haber DA, Li E. DNA methyltransferases Dnmt3a and Dnmt3b are essential for de novo methylation and mammalian development. Cell. 1999; 99:247–257. [PubMed: 10555141]

48. Subramaniam D, Thombre R, Dhar A, Anant S. DNA methyltransferases: a novel target for prevention and therapy. Front Oncol. 2014; 4:80. [PubMed: 24822169]

49. Xu Z, Zeng X, Xu J, Xu D, Li J, Jin H, et al. Isorhapontigenin suppresses growth of patient-derived glioblastoma spheres through regulating miR-145/SOX2/cyclin D1 axis. Neuro-oncology. 2016; 18:830–839. [PubMed: 26681767]

50. Huang H, Pan X, Jin H, Li Y, Zhang L, Yang C, et al. PHLPP2 Downregulation Contributes to Lung Carcinogenesis Following B[a]P/B[a]PDE Exposure. Clinical cancer research : an official journal of the American Association for Cancer Research. 2015; 21:3783–3793. [PubMed: 25977341]

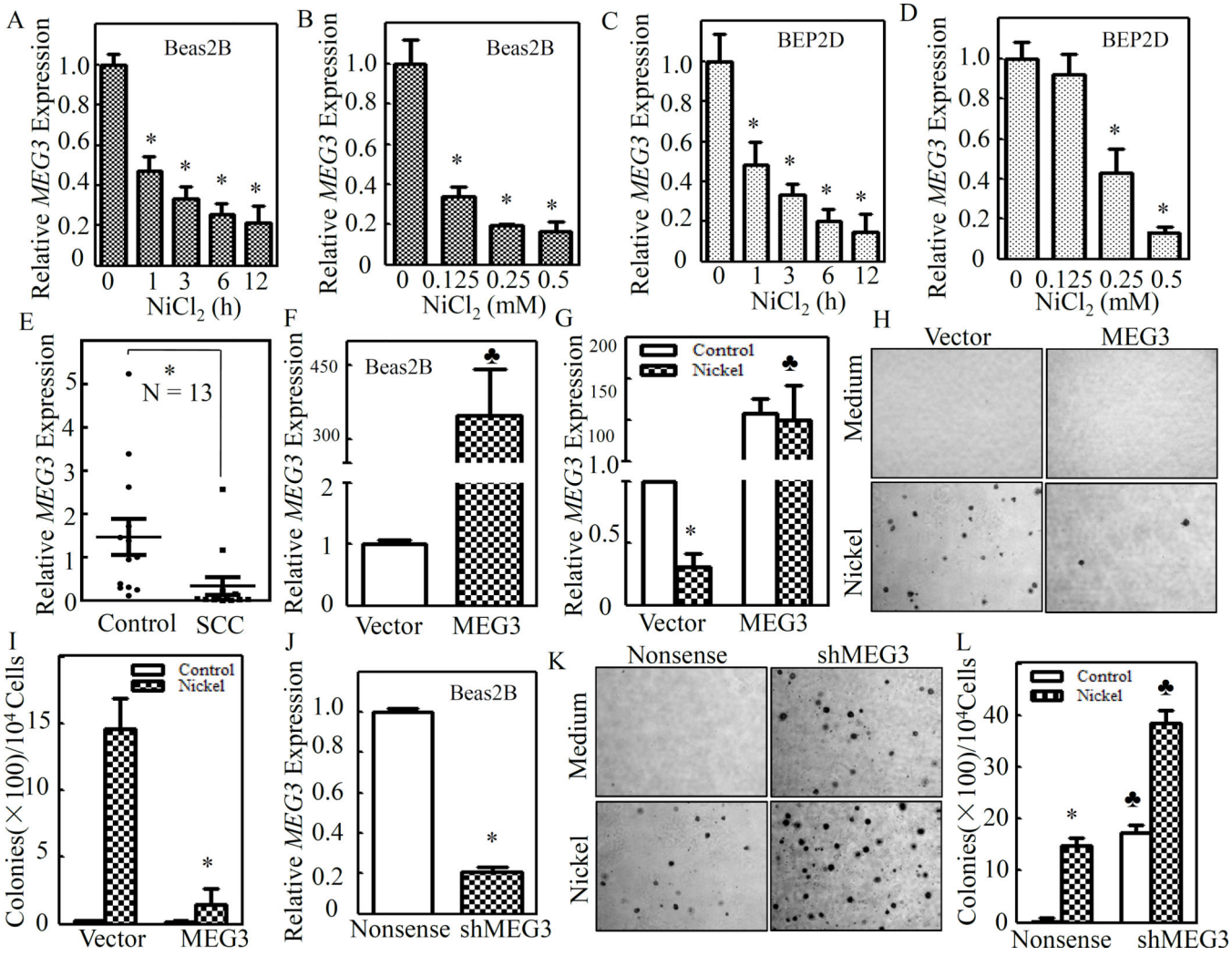

Figure 1. Nickel-induced *MEG3* downregulation contributed to malignant transformation of Beas2B cells

(A – D) Beas2B or BEP2D cells (2×10^5) were seeded into each well of 6-well plates and cultured till the cell density reached 80–90%. The cells were then exposed to 0.5 mM of $NiCl_2$ for the indicated time periods (A & C) or to various concentrations of NiCl2 for 12 h (B & D). (E) Thirteen pairs of human primary lung squamous cell carcinomas and their adjacent normal lung tissues were obtained from the First Affiliated Hospital of Wenzhou Medical University. The relative levels of *MEG3* were determined by qPCR using gene specific primers as described in the section of "Materials and Methods", and *gapdh* was measured as an internal control. (F) *MEG3* overexpression was identified in Beas2B(MEG3) in comparison to Beas2B(Vector) cells. The spade (♣) indicates a significant increase in comparison to Beas2B(Vector) cells ($P< 0.05$). (G) Nickel exposure resulted in downregulation of endogenous *MEG3*, but not ectopically expressed *MEG3*. The asterisk (*) indicates a significant decrease in comparison to medium control ($P< 0.05$). The spade (♣) indicates a significant increase in comparison to Beas2B(Vector) ($P< 0.05$). (H&I) Beas2B(MEG3) and Beas2B(Vector) were repeatedly exposed to 0.5 mM of $NiCl_2$ for 3 months and the nickel treated cells were subjected to anchorage-independent assay in soft

agar (H). The number of colonies were scored and presented as colonies per 10^4 seeded cells (I). The asterisk (*) indicates a significant decrease in comparison to Beas2B(Vector) ($P< 0.05$). (J) shMEG3 knockdown plasmid was stably transfected into Beas2B cells and the stable transfectants were identified. The asterisk (*) indicates a significant decrease in comparison to Beas2B(Nonsense) ($P< 0.05$). (K&L) Beas2B(shMEG3) and Beas2B(Nonsense) cells were repeatedly exposed to 0.5 mM of $NiCl_2$ for 3 months and nickel treated cells were subjected to anchorage-independent growth assay (K). The number of colonies were scored and presented as colonies per 10^4 seeded cells (L). The asterisk (*) indicates a significant decrease in comparison to medium control ($P< 0.05$;left). The spade (♣) indicates a significant increase in comparison to Beas2B(Nonsense) cells ($P< 0.05$).

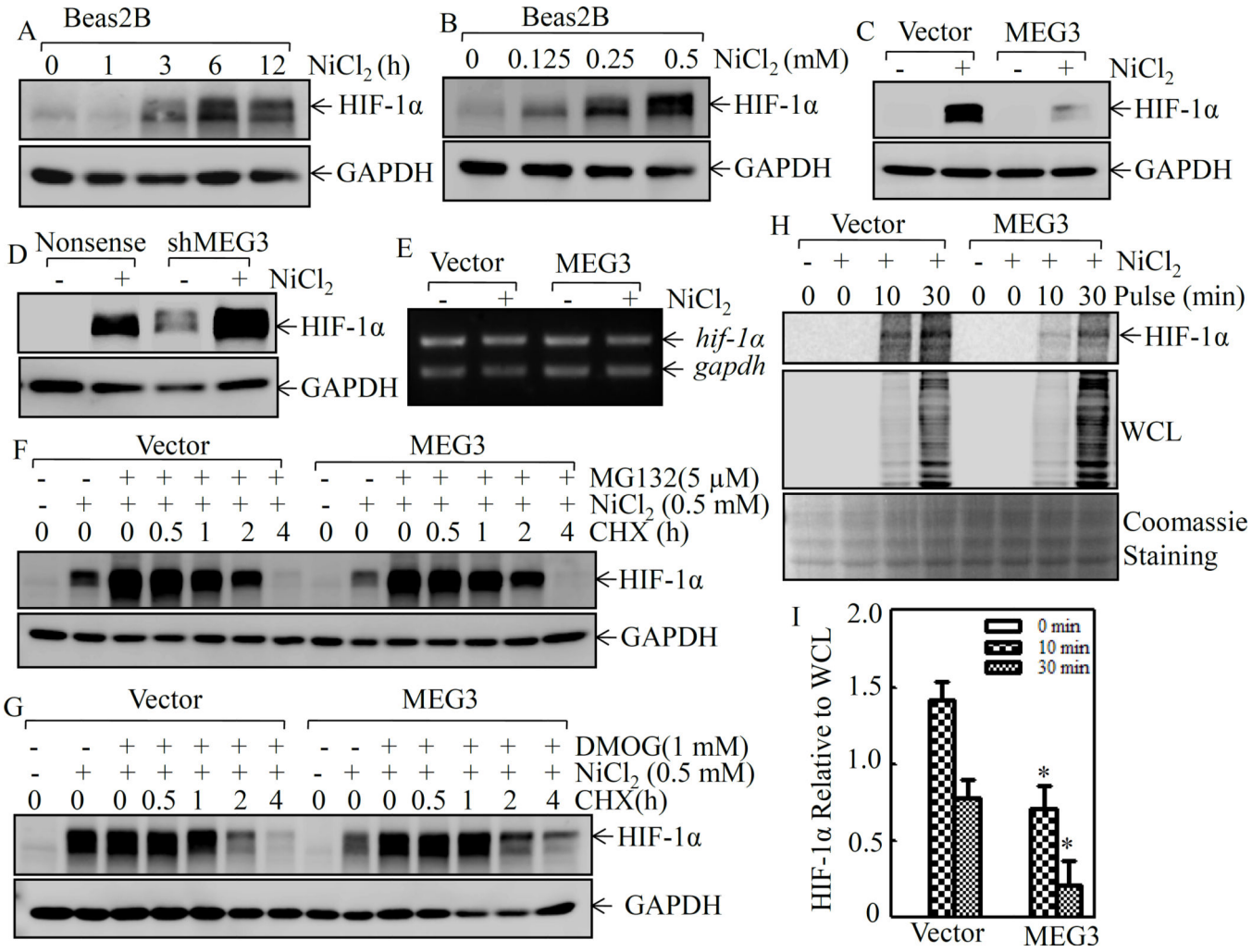

Figure 2. *MEG3* inhibited HIF-1α protein translation in Beas2B cells

(A & B) Beas2B cells were exposed to 0.5 mM of $NiCl_2$ for the indicated time periods(A) or to various doses of $NiCl_2$ for 6 h(B). The extracts were subjected to Western blotting to determine HIF-1α protein expression. GAPDH was used as a protein loading control. (C & D) Beas2b(MEG3) vs. Beas2B(Vector) (C) or Beas2B(shMEG3) vs. Beas2B(Nonsense) cells (D) were exposed to 0.5 mM of $NiCl_2$ for 6 h. The cell extracts were subjected to Western blotting for determination of HIF-1α protein expression. (E) Beas2B(MEG3) and Beas2B(Vector) cells were exposed to 0.5 mM of $NiCl_2$ for 6 h and the cells were then used to extract total RNA using Trizol reagent. RT-PCR was carried out to detect *hif-1α* mRNA expression. gapdh was used a loading control. (F & G) Beas2B(MEG3) and Beas2B(Vector) cells were pre-treated with $NiCl_2$ plus MG132 (F) or NiCl2 plus DMOG (G) for 6 h. The cells were then used to determine of HIF-1α protein degradation rates in the presence of cycloheximide (CHX; 50μg/mL) for different time periods. (H & I) Beas2B(MEG3) and Beas2B(Vector) cells were exposed to 0.5 mM of $NiCl_2$ for 6 h. The newly synthesized HIF-1α protein was monitored by pulse assay using [^{35}S]-labeled methionine-cysteine. WCL stands for whole cell lysate and Coomassie blue staining was used for protein loading

control (H). The content of the newly synthesized HIF-1α protein was normalized to the total newly synthesized protein (I).

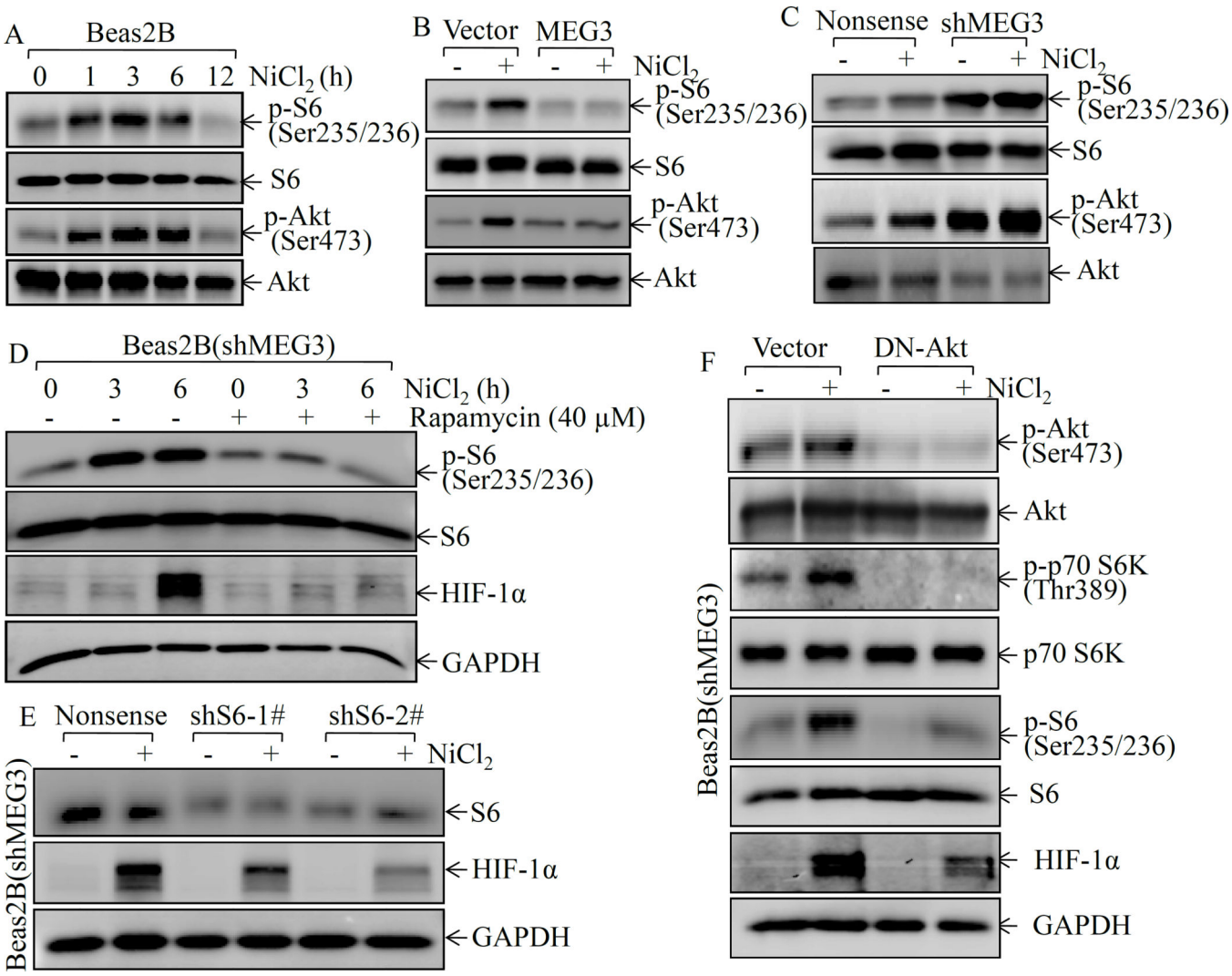

Figure 3. *MEG3* inhibited nickel-induced HIF-1α protein expression by targeting Akt/p70S6K/S6 ribosomal pathway

(A) Beas2B cells were exposed to 0.5 mM of $NiCl_2$ for the indicated time periods. The cell extracts were subjected to Western blotting to determine p-S6 phosphorylation at Ser235/236, S6, Akt phosphorylation at Ser473, and Akt. (B & C) Beas2B(MEG3) vs. Beas2B(Vector) or Beas2B(shMEG3) vs. Beas2B(Nonsense) cells were exposed to 0.5 mM of $NiCl_2$ for 6 h. The cell extracts were subjected to Western blotting to determinate p-S6 phosphorylation at Ser235/236, S6, Akt phosphorylation at Ser473, and Akt. (D) Beas2B(shMEG3) cells were pretreated with rapamycin (40μM) for 30min, the cells were then exposed to 0.5 mM of $NiCl_2$ for the indicated time periods. The cell extracts were subjected to Western blotting to determinate p-S6 phosphorylation at Ser235/236, S6, HIF-lα, and GAPDH protein expression. (E) shRNA specific targeting S6 and its scramble control were transiently transfected into Beas2B cells and the transfectants were exposed to 0.5 mM of $NiCl_2$ for 6 h. The cell extracts were subjected to Western blotting to determinate S6, HIF-lα, and GAPDH protein expression. (F) DN-AKT plasmid and its scramble control were transiently transfected into Beas2B(shMEG3) cells. The transfectants were exposed to

0.5 mM of $NiCl_2$ for 6 h and then were extracted to determinate Akt phosphorylation at Ser473, Akt, p70S6K phosphorylation at Thr389, p70S6K, S6 phosphorylation at Ser235/236, S6, HIF-1α, and GAPDH by Western blot.

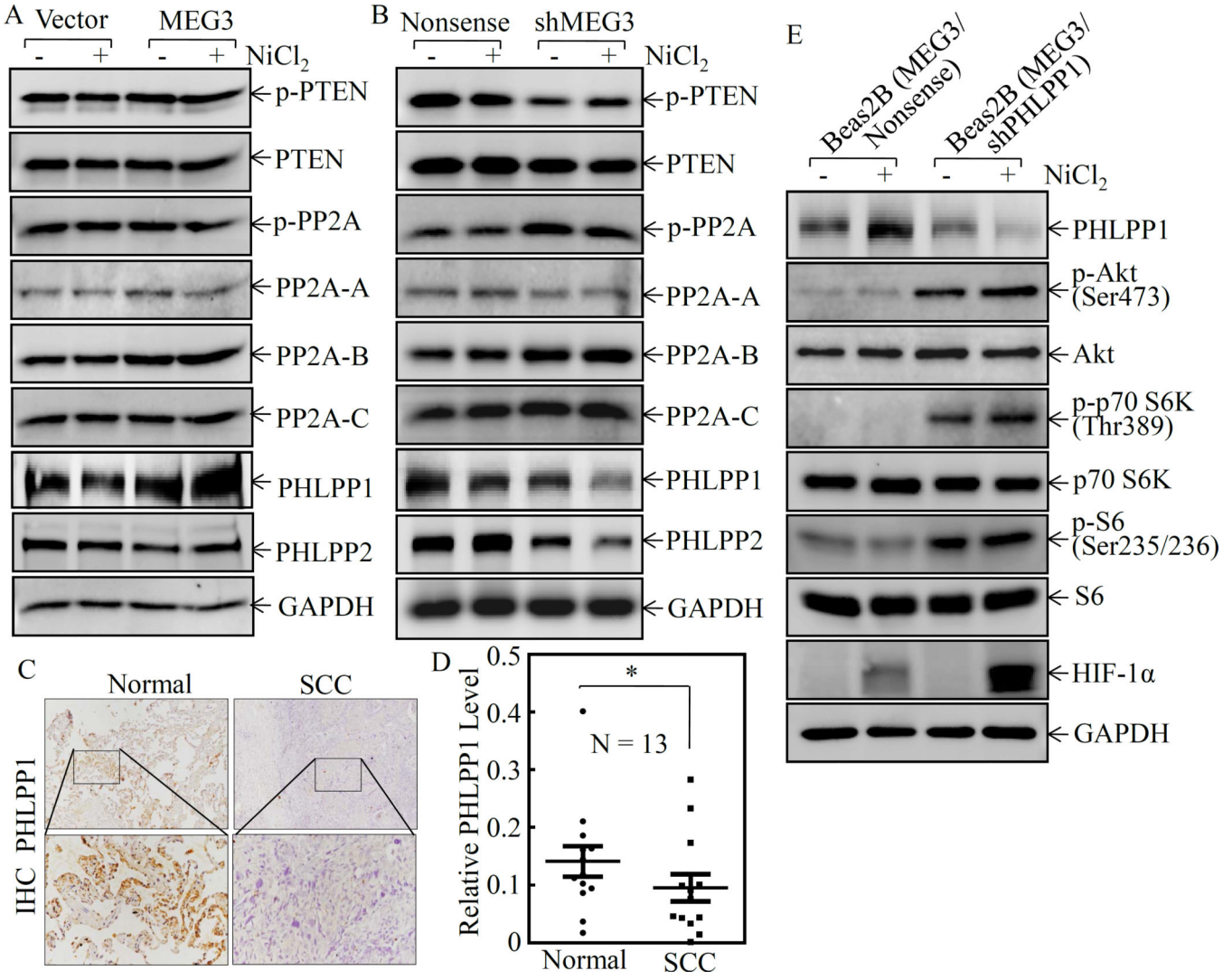

Figure 4. PHLPP1 contributed to the activation of Akt/p70S6K/S6 ribosomal pathway and induction of HIF1α protein

(A & B) Beas2B(MEG3) vs. Beas2B(Vector) or Beas2B(shMEG3) vs. Beas2B(Nonsense) cells were exposed to 0.5 mM of $NiCl_2$ for 6 h. The cell extracts were subjected to Western blotting for determining PHLPP1, PHLPP2, p-PP2A, PP2A-A, PP2A-B, PP2A-C, p-PTEN, PTEN, and GAPDH protein expression. (C&D) PHLPP1 expression in human lung squamous cell carcinomas was evaluated by IHC staining (C) and analyzed by calculating the integrated optical density per stained area (IOD/area) (D). (E) shRNA targeting PHLPP1 and its scramble control plasmids were transiently transfected into Beas2B(MEG3) cells and the transfectants were exposed to 0.5 mM of $NiCl_2$ for 6 h. The cells were then extracted to determinate PHLPP1, Akt phosphorylation at Ser473, Akt, p70S6K phosphorylation at Thr389, p70S6K, S6 phosphorylation at Ser235/236, S6, HIF-lα, and GAPDH by Western blotting.

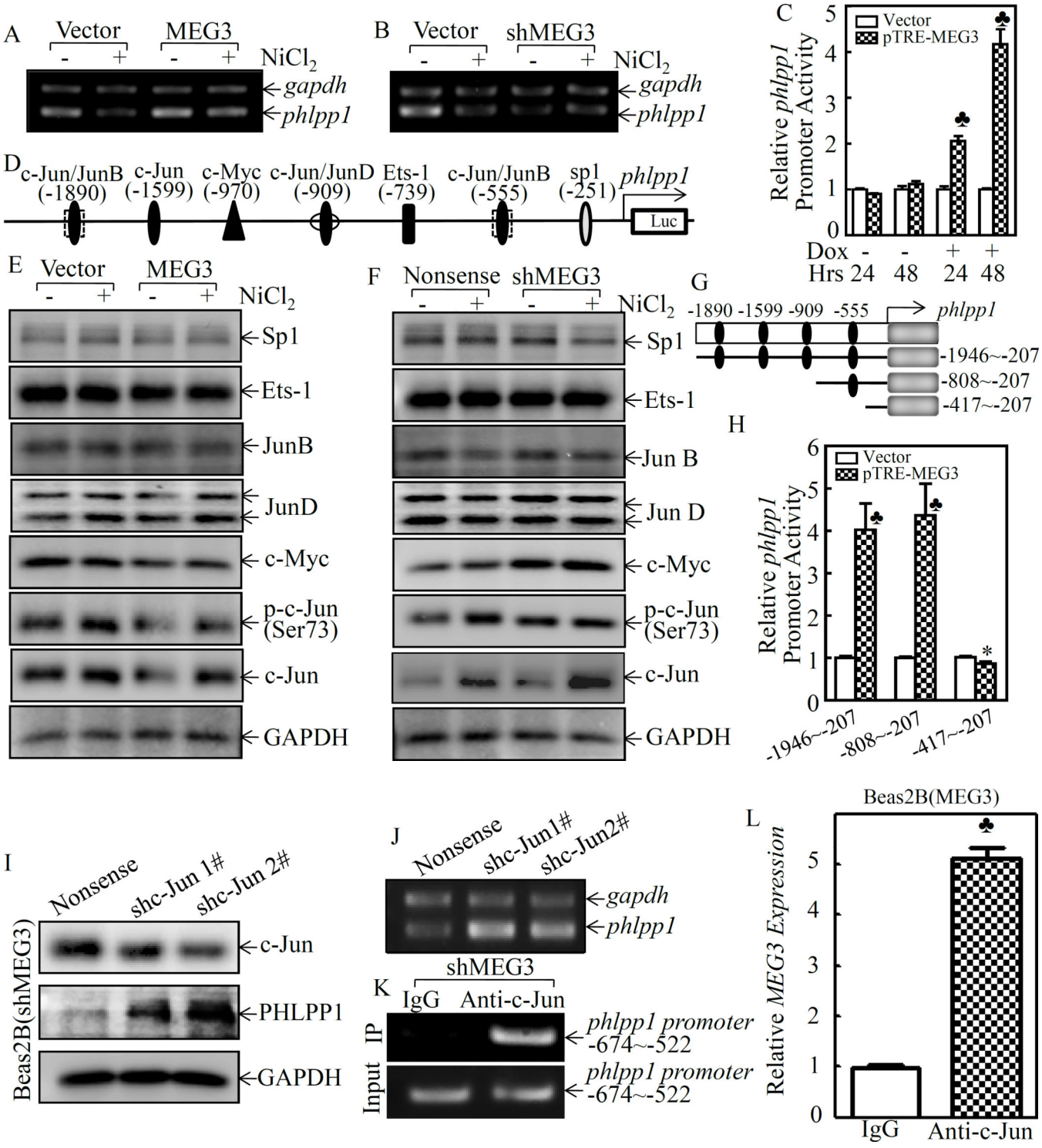

Figure 5. *MEG3* interacted with transcription factor c-Jun, consequently regulating PHLPP1 promoter transcription

(A & B) Beas2B(MEG3) vs. Beas2B(Vector) or Beas2B(shMEG3) vs. Beas2B(Nonsense) cells were exposed to 0.5 mM of NiCl2 for 6 h. The cells were then used to extract total RNA using Trizol reagent. RT-PCR was carried out to detect *phlpp1* mRNA expression and

gapdh was used as a loading control. (C) the full long *phlpp1* promoter-driven luciferase reporter constructs co-transfected with TK into Beas2B(pTRE-MEG3) and Beas2B(Vector), respectively. (D) The potential transcriptional factor binding sites in PHLPP1 promoter region (−2000~+0) were analyzed using the TRANSFAC 8.3 engine online. (E & F) Beas2B(MEG3) vs. Beas2B(Vector) or Beas2B(shMEG3) vs. Beas2B(Nonsense) cells were exposed to 0.5 mM of $NiCl_2$ for 6 h. The cell extracts were subjected to Western blotting to determinate p-c-Jun(Ser73), c-Jun, sp1, Ets-1, JunB, JunD, and c-Myc. GAPDH was used as a protein loading control. (G) A schematic illustration of the construction of *phlpp1* promoter-driven luciferase reporter constructs. (H) The various *phlpp1* promoter-driven luciferase reporter constructs together with TK were stably transfected into Beas2B(pTRE-MEG3) and Beas2B(Vector), respectively. The transfectants were extracted to evaluate the luciferase activity after 48 h and the results are presented as relative *phlpp1* promoter activity by normalization of luciferase activity to Renilla luciferase activity. The spade (♣) indicates a significant increase in comparison to the vector control group ($P< 0.05$) and the asterisk (*) indicates a significant decrease in comparison to other phlpp1 promoter-driven luciferase reporters ($P< 0.05$). (I) shRNA targeting c-Jun and its scramble control plasmid was transiently transfected into Beas2B(shMEG3) cells and the transfectants were extracted to determinate c-Jun, PHLPP1, and GAPDH by Western blot. (J) The cell transfectants were used to extract total RNA and *phlpp1* expression was evaluated by using RT-PCR. (K) ChIP assays were performed to determine c-Jun binding to the *phlpp1* promoter in Beas2B(shMEG3) cells, as described in the section of “Materials and Methods”. (L) RNA-IP was carried out to evaluate specific interaction of *MEG3* with c-Jun. The spade (♣) indicates a significant increase in comparison to IgG control group ($P< 0.05$).

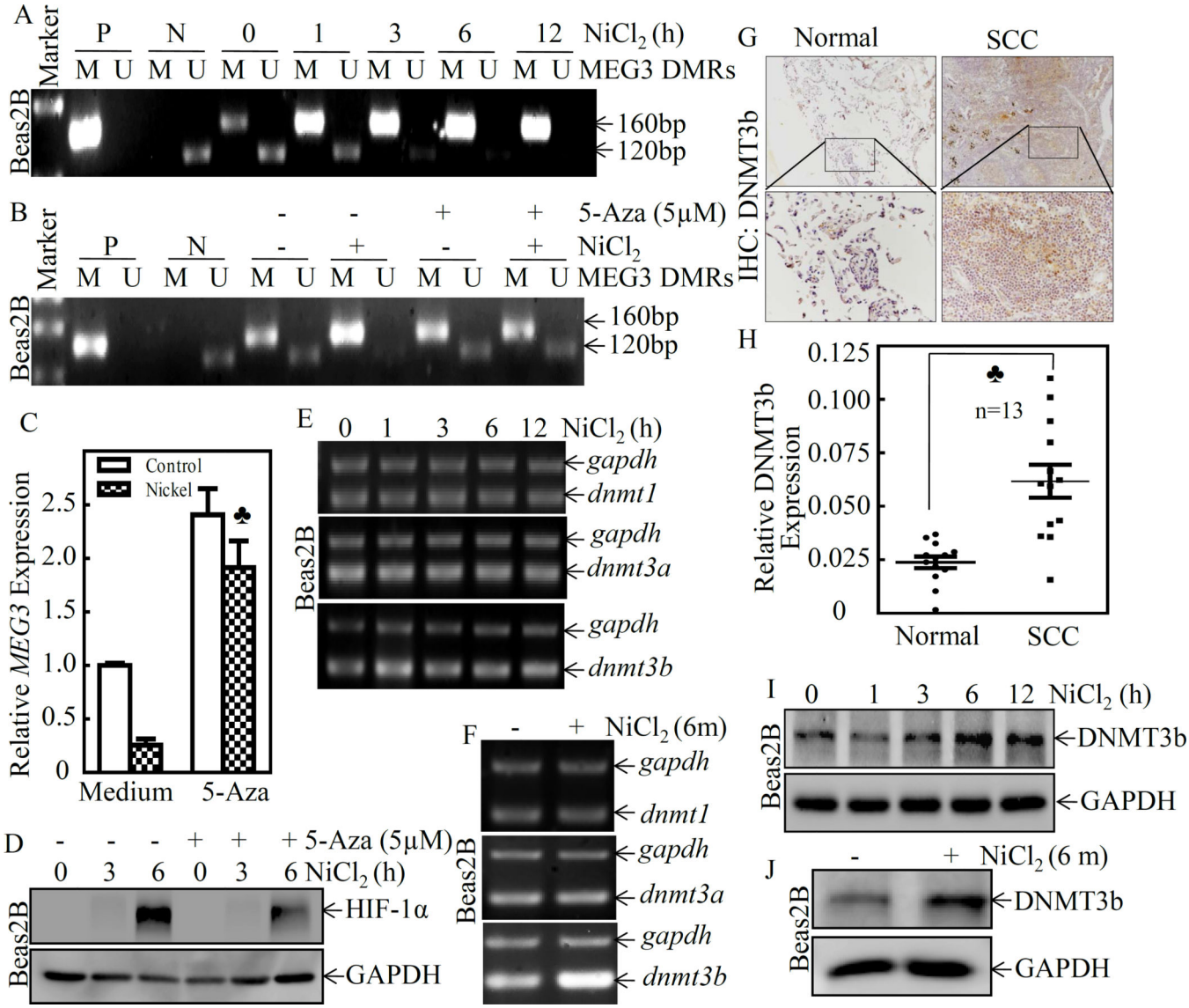

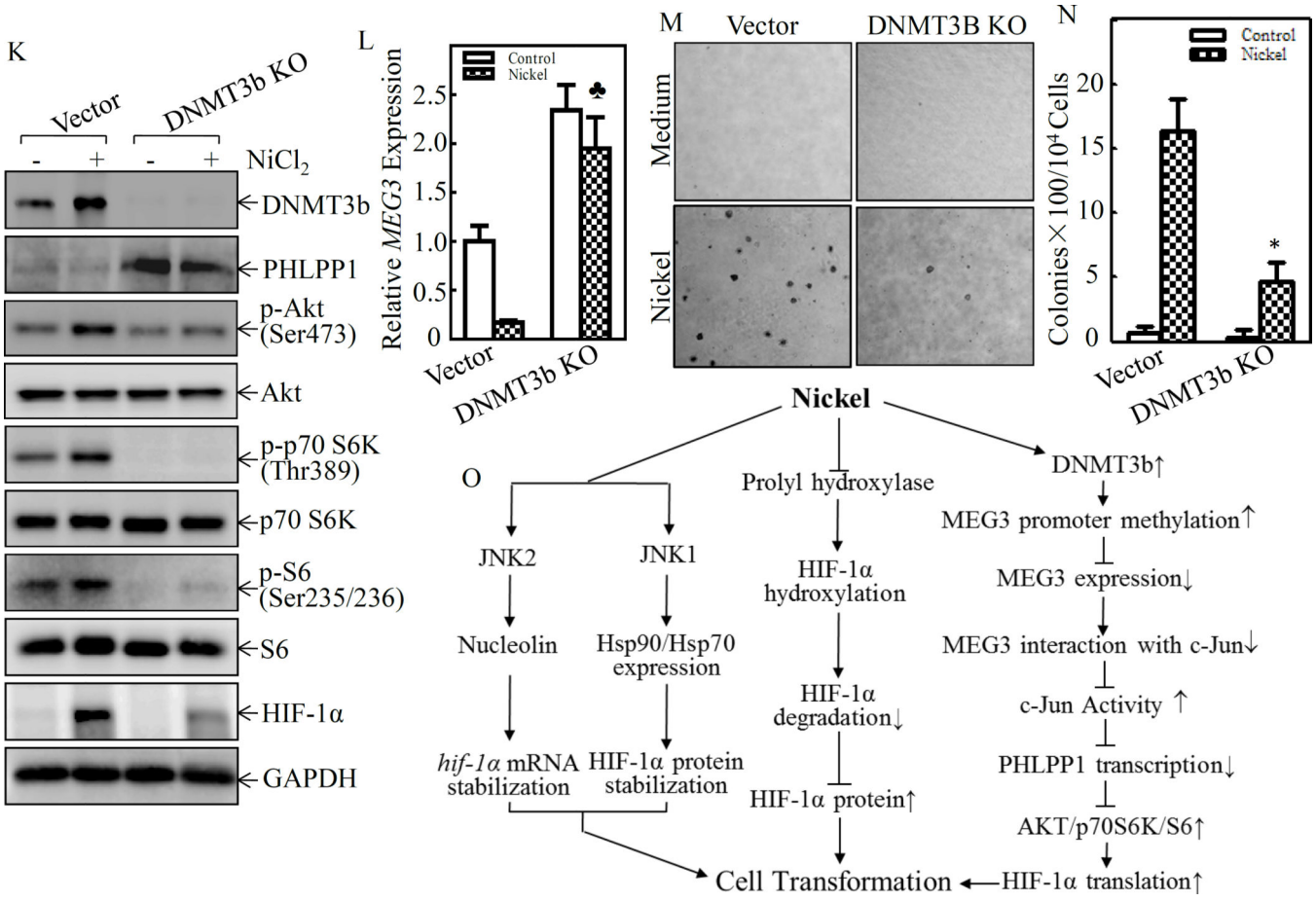

Figure 6. DNMT3b mediated promoter hypermethylation contributed to *MEG3* downregulation and HIF-1α protein expression following nickel exposure

(A) Beas2B cells were exposed to 0.5 mM of $NiCl_2$ for the indicated time periods. The methylation status of the *MEG3* promoter in the differentially methylated region (DMR) was determined using the methylation-specific PCR (MS-PCR) assay. A primer set was used to evaluate the methylated (M) and unmethylated (U) copies of the *MEG3* DMR gene. Methylated control was used as the positive control (P), while unmethylated control was used as the negative control (N) A 160 bp PCR product represents the methylated state and a 120 bp PCR product stands for the unmethylated allele. (B–D) Beas2B cells were pretreated with 5-aza-2'-deoxycytidine (5μM) for 72h, then exposed to 0.5 mM of $NiCl_2$ for 6h. The cells were extracted to determinate the methylation status of the *MEG3* promoter DMR by using the MS-PCR (B). The relative levels of *MEG3* were determined by qPCR using gene specific primers and *gapdh* was used as an internal control. The spade (♣) indicates a significant increase in comparison to the medium control ($P< 0.05$) (C). The cells were also extracted for determination of HIF-1α and GAPDH protein expression by Western Blot (D). (E & F) Beas2B cells were exposed to 0.5 mM of $NiCl_2$ for the indicated time periods and total RNA was extracted to detect *dnmt1, dnmt3a*, and *dnmt3b* expression using RT-PCR. (G & H) Immunohistochemically staining was carried out to evaluate DNMT3b expression in human lung squamous cell carcinomas and protein expression levels were analyzed by calculating the integrated optical density per stained area (IOD/area). (I & J) Beas2B cells

were exposed to 0.5 mM of $NiCl_2$ for the indicated time periods and the cells were extracted to determinate the DNMT3b and GAPDH protein expression by Western Blot. (K) DNMT3B CRISP knockout cell, Beas2B(DNMT3B KO), and its scramble control transfectant, Beas2B(Vector) cells, were exposed to 0.5 mM of $NiCl_2$ for 6 h. The cell protein extracts were subjected to Western blot to determinate protein expression, as indicated (K), mRNA extracts were subjected to determinate *MEG3* by qPCR (L). (M & N) Beas2B(DNMT3B KO) and Beas2B(Vector) cells and were repeatedly exposed to 0.5 mM of $NiCl_2$ for 3 months. The cells were than subjected to determinate the anchorage-independent growth capability in soft agar (M). The number of colonies were scored and presented as colonies per 10^4 seeded cells (N). The asterisk (*) indicate a significant decrease in comparison to Beas2B(Vector) cells ($P< 0.05$). (O) A schematic illustration of the role and molecular mechanism underlying *MEG3* in promotion of HIF-1α protein translation and malignant transformation of human bronchial epithelial cells following nickel exposure.